J Mater Sci (2010) 45:850–858
DOI 10.1007/s10853-009-4009-3

Characterization and wear behavior of plasma-sprayed Al_2O_3 and ZrO_25CaO coatings on cast iron substrate

N. Krishnamurthy · M. S. Murali · P. G. Mukunda · M. R. Ramesh

Received: 4 August 2009 / Accepted: 29 October 2009 / Published online: 12 November 2009

Abstract Plasma spraying is one of the methods used for combating wear. Despite of its wide spread industrial use, little is known about the basic friction behavior and mechanism by which such coatings wear. In this work, the abrasive wear resistance of plasma-sprayed ceramic coatings on cast iron substrate has been investigated through pin-on-disc test. It was found that the coefficient of friction and wear affected mainly by splats and porosity, surface roughness, and coating thickness. The coefficient of friction is found to be more significantly affected by load than by other test parameters. This work also includes the characterization of coatings.

Introduction

Due to market pressures for improvements in productivity, reliability, durability, wear resistance as well as the profitability of mechanical systems, manufacturers are placing increasing demands on the available materials. Economic constraints require that these materials be inexpensive and be easily available. In order to enhance the surface properties of today's materials, producers of components are turning to different surface treatments and in particular to hard protective coatings [1]. Thermal Barrier Coatings (TBCs) have been used extensively as one of the hard protective coatings for so many engineering components [2–7]. TBCs are used to improve fuel efficiency by insulating the combustion chamber components of an engine, there by recovering 8–15% of the energy that is attributed to heat losses. These coatings have been applied to the cylinder head, the valves, the piston and liner, etc.

Thermal barrier and wear resistant coatings are produced using thermal spraying method which is often considered as a potential alternative to traditional coating manufacturing techniques such as hard chrome electroplating, Physical Vapor Deposition (PVD), Chemical Vapor Deposition (CVD), etc. [8–10]. Among various thermal spraying techniques, plasma spraying has been widely employed to provide an improved wear resistance to various industrial parts [11–15]. The plasma-sprayed ceramic coatings possess very high hardness. Due to their purely ceramic nature, they are almost insensitive to many corrosive environments and can withstand high temperatures [16]. These coatings are made up of layers that are formed when melted material droplets flatten and solidify on the surface of the substrate [17]. Because of their lamellar structure, the coatings have various amounts of internal stresses. This internal stress and incomplete bonding between lamellae decrease the strength, wear resistance, and the corrosion resistance of the coatings. The variety of defects present in plasma-sprayed coatings make the modeling of wear properties difficult. However it has been shown that coatings with more homogeneous and denser structure perform better than badly structured coatings in abrasion. Inhomogeneities tend to cause local fractures. The coupling between hardness and wear resistance is often unclear, presumably because of the low fracture toughness [18, 19]. The wear behavior of plasma-sprayed Al_2O_3 coatings conducted in a block-on ring tester

N. Krishnamurthy (✉) · P. G. Mukunda
Nitte Meenakshi Institute of Technology, Bangalore, India
e-mail: krishamu@rediffmail.com

M. S. Murali
R.V. College of Engineering, Bangalore, India

M. R. Ramesh
Reva Institute of Technology and Management, Bangalore, India

was reported to be dominated by plastic deformation and adhesive wear as well as brittle fracture [20].

Zirconia-based ceramics have been used in engines and gas turbines as thermal barrier coatings. Plasma spraying of these materials could enhance the thermal efficiency [21–26] of internal combustion engines and increase the service life of piston ring or cylinder liner pairs. Zirconia coatings are interesting materials because of their outstanding mechanical, thermal, optical, and electrical properties. They have high melting points, high resistance to oxidation, low thermal conductivity and high co-efficient of thermal expansion.

A thorough study of the wear resistance of thermally sprayed coatings must involve plasma-sprayed ceramics, which could represent an economical alternative to High Velocity Oxygen Fuel (HVOF)-sprayed cermets in some industrial applications. Much research related to the basic wear mechanisms of plasma-sprayed oxides exist, since such coatings have been studied for a long time [20, 27–29], however there exist a few reports comparing them to the characteristics of other thermally sprayed coatings as well as to other industrially used wear resistant coatings such as hard chrome electroplating and nickel electroless plating [30, 31]. The tribological behavior of the coatings is closely linked to the microstructure [32–34].

The main objective of this investigation is to provide an experimental data of the wear rates, wear mechanisms, friction coefficients of Al_2O_3 and ZrO_25CaO plasma-sprayed coatings under different load conditions and dry environment.

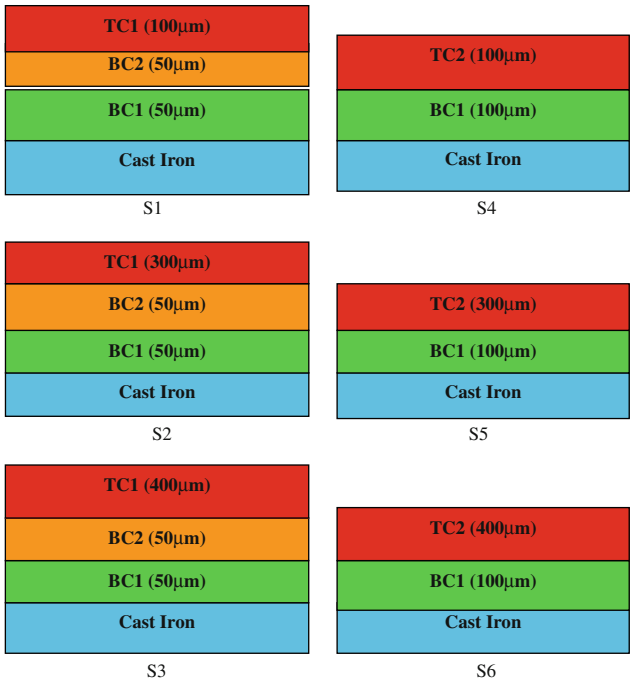

Fig. 1 Schematic diagram of samples

Experimental details

Plasma spraying

Cast iron circular pins of diameter 12 mm and length 25 mm were selected as substrate material for coating. The composition of cast iron substrate material is given in Table 1.

The substrate component was checked for dimensional accuracy and surface finish. Then substrates were degreased by immersing in a vapor bath of tetra chloroethylene boiled at 70–80 °C to remove grease. The surfaces to be coated were grit blasted using Al_2O_3 grains (−18 + 24 mesh) with a pressure of 455 kPa. The trade names and chemical compositions of bond and top coat powders are given in Table 1. The schematic diagram of coating layers and their thicknesses are shown in Fig. 1. The coating process was accomplished with a Sulzer Metco plasma spraying equipment. The spray parameters for different materials are shown in Table 2.

Material characterization

Measurement of surface texture parameters

For each specimen, surface texture parameters were measured using Mahr Perthometer. For this measurement, first the coated surface of each specimen was divided into 10 × 10 mm^2. The tracing length was kept at 5.6 mm. For each element the parameters like arithmetical mean

Table 1 Chemical composition of substrate and coating materials

Substrate material			
Cast iron			
Fe-3.54, C-2.21, Si-0.67, Mn-0.25, Cr-0.013, Cu-0.56, P-0.031			
Coating material			
Metco105SFP (TC1)	Metco 201NS(TC2)	Metco 452(BC1)	Metco 410NS(BC2)
99.5 Al_2O_3	ZrO_2 5CaO	Fe 38Ni10Al	Al_2O_330(Ni 20Al)

TC1 Top coat 1, *TC2* Top coat 2, *BC1* Bond coat 1, *BC2* Bond coat 2

Table 2 Plasma spray parameters for different coating materials used

Materials	Primary gas (Argon) pressure (kPa)	Secondary gas (H_2) pressure (kPa)	Carrier gas (Argon) flow (lpm)	Current (A)	Voltage (V)	Spray distance (mm)	Feed rate (kg/h)
TC1	700	520	60	600	65	64–125	2.7
TC2	345	345	37	500	75	50–100	5.4
BC1	700	340	37	500	65	100–175	4.1
BC2	700	350	37	500	65	75–125	2.3

deviation or average roughness (R_a) were recorded. A 3D map was drawn for each coated specimen taking average roughness in vertical coordinate. Microstructures of coatings and surface morphology were studied using JOEL-JAPAN JSM-840A scanning electron microscope.

The porosity of each component was also noted.

Tribological testing

Friction and wear tests were carried out on coated specimens using DUCOM Pin-on Disk tribometer. A 60 grit Al_2O_3 abrasive wheel was used as disk. The specification of the wheel is WA60K5V. Three tests were performed on each sample under 5, 10, and 15 N normal loads. A track diameter of 80 mm and a speed of 200 rpm under atmospheric conditions were used for the test. The sliding distance was kept constant at 378 m. For each applied load, wear rate and coefficient of friction were recorded.

Results and discussion

Coating characterization

Scanning electron micrographs of Al_2O_3 coatings S1, S2, and S3 (Fig. 2) are characterized by the existence of disk-shaped grains. These grains are formed by the molten droplets of coating material, flattened on impact on the substrate. The molten particles were distributed more or less evenly producing a smooth surface. Coatings also reveal partly melted particles of the coating powders. The SEM images of Al_2O_3 coatings (Fig. 3) show pores with a diameter of 2–5 μm.The images of other Al_2O_3 coatings are also similar in appearance. Pores are observed both in bond and top coats. They are distributed unevenly in bond coat and more evenly in top coat. The porosity in these coatings lies in the range of 5–6%. It is high, due to more rounded pores produced by unmelted particles, splats, stacking faults, and gas entrapment. The enlarged view of the marked region of S1 showed a network of microcracks. Cracks are also observed on the surface of flattened droplets. Residual stress by thermal shock during spray process resulted in trans-granular microcracks in the coatings. The increase in thickness of top coat has less effect on microstructure as shown in S2 and S3. But the porosity of coatings increases slightly with increase in coating thickness.

The SEM structure of ZrO_25CaO coatings S4, S5, S6 (Fig. 2) shows a dense structure of mounds. Similar to Al_2O_3 coatings, these also show the existence of unmelted and partly melted particles. The size of the micro crack is slightly more than that of Al_2O_3 coatings. It is mainly due to the low thermal conductivity of ZrO_25CaO compared to that of cast iron substrate. The thermal conductivity of ZrO_25CaO is about 2–4 W/mK, where as cast iron has about 50–55 W/mK. The heat generated during spraying process being accumulated in the ZrO_25CaO layer which inturn increases the thermal stresses inside the coating producing cracks with bigger size. But in case of alumina coatings the difference in thermal conductivity between substrate and top coat is less (thermal conductivity of alumina is 33–37 W/mK) which enables more heat to flow out of the coating reducing thermal stresses. The splats in the coatings are separated by inter-lamellar pores resulting from rapid solidification of the lamellae, very fine voids formed by incomplete inter-splat contact or around unmelted particles. The porosity of ZrO_25CaO coatings lies in the range of 6–8%. Here also the increase in top coat thickness has less effect on microstructure as shown in S5 and S6 (Fig. 2). But the porosity of these coatings increases slightly with increase in top coat thickness (7.5–8%).

Figure 4 shows the 3D profile of average roughness (R_a) for S1 and S6 samples (similar graphs are obtained for S2, S3, S4, and S5 but not shown in figure). From the 3D-maps, it is observed that the average roughness R_a varies from 3.5 to 5.5 μm in the case of alumina coatings and 4.5 to 6.8 μm for ZrO_25CaO coatings. As discussed in microstructure, the top coat of S4, S5, and S6 possesses mounds of molten and unmolten particles which lead to increase in roughness. The flowability of zirconia is less compared to alumina which also leads to formation of mounds and they affect the surface texture of coating.

Friction coefficient and wear rates

Load or contact stress is the most obvious and easily monitored parameter that can affect wear. The magnitude of the normal load or the contact stress is important since it increases both the area of contact and the depth below the

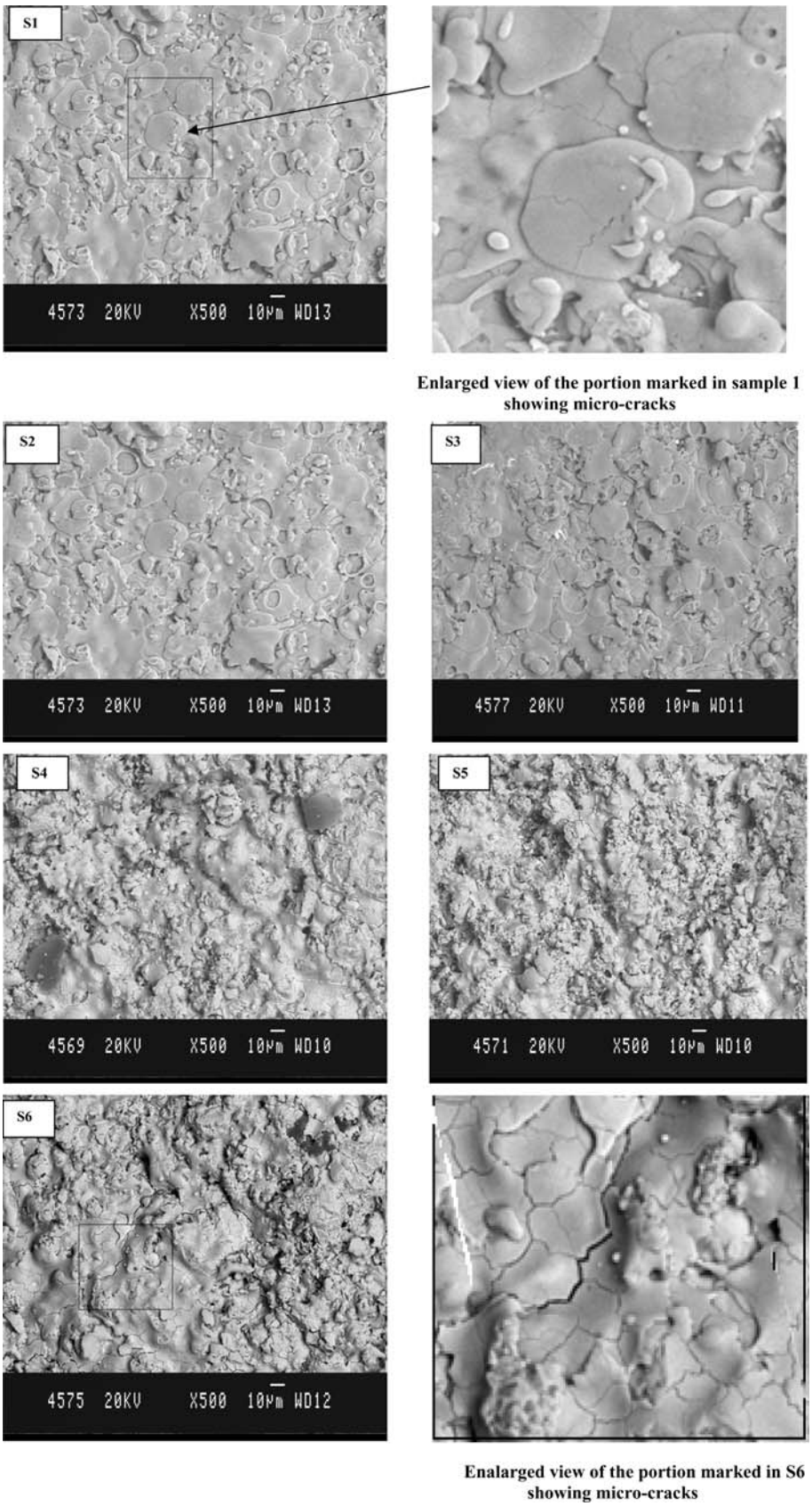

Fig. 2 Scanning electron micrographs showing morphology of S1, S2, S3, S4, S5, and S6 samples

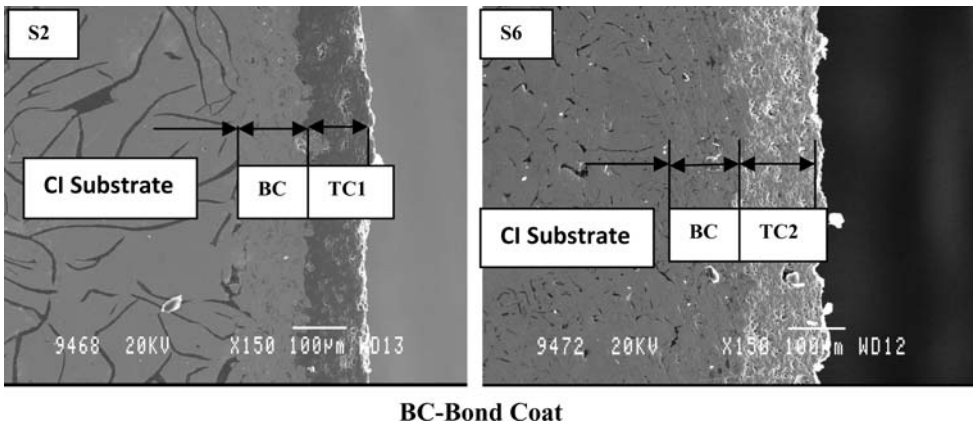

Fig. 3 SEM micrographs showing cross section of coatings for S2 and S6

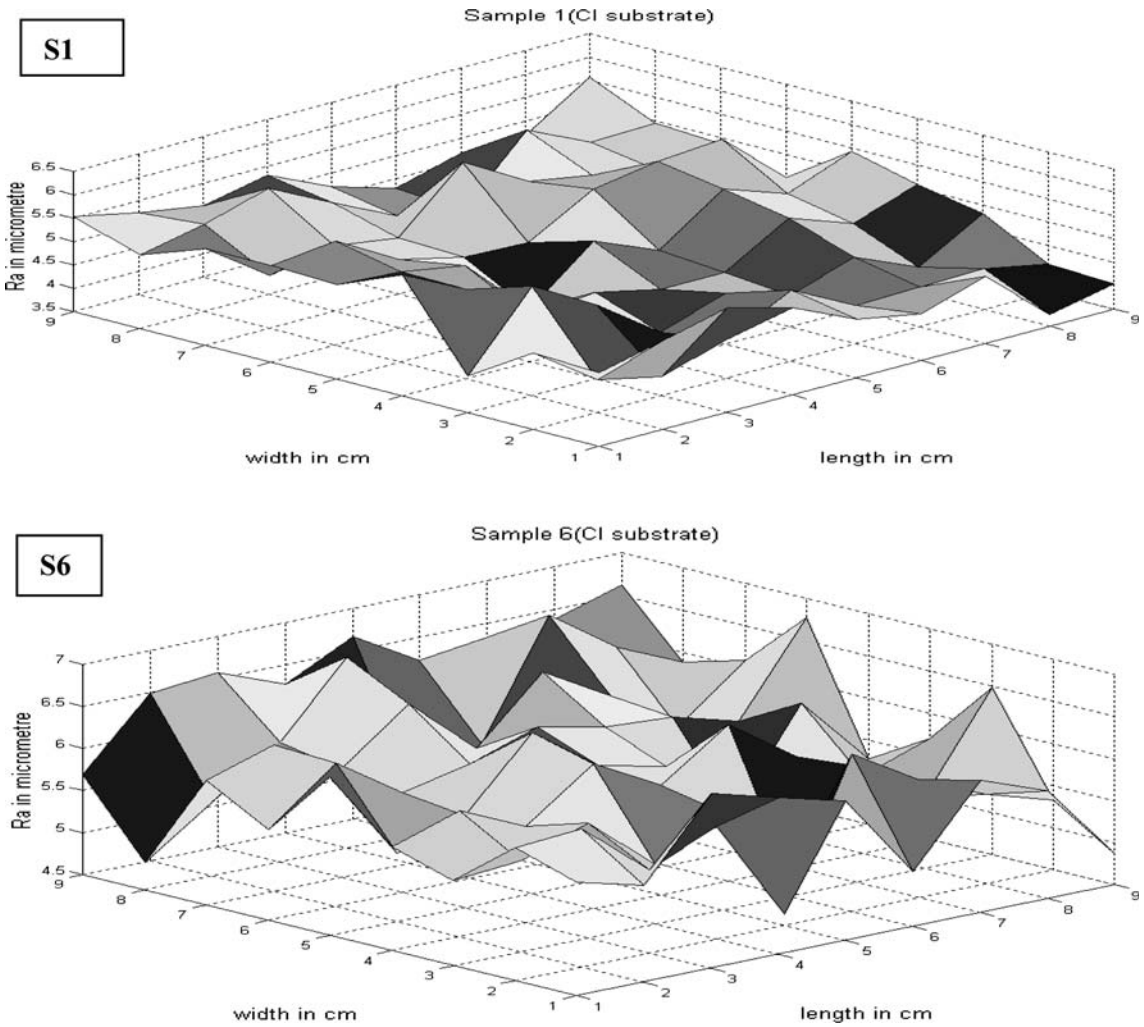

Fig. 4 3D maps with average surface roughness R_a as the criteria for S1 and S6

surface at which the maximum shear stress occurs as well as elastic or plastic deformation state. Assessments of the friction coefficient against loads of 5, 10, and 15 N under dry conditions are shown in Figs. 5, 6, and 7, respectively. It is found that there is a very short period of an increase in friction coefficient related to a running-in-step followed by a decrease. After the decrease, the coefficient of friction almost remains the same for some period and again increases till the end of cycle. This trend is similar for all samples under a given load conditions. At the beginning of

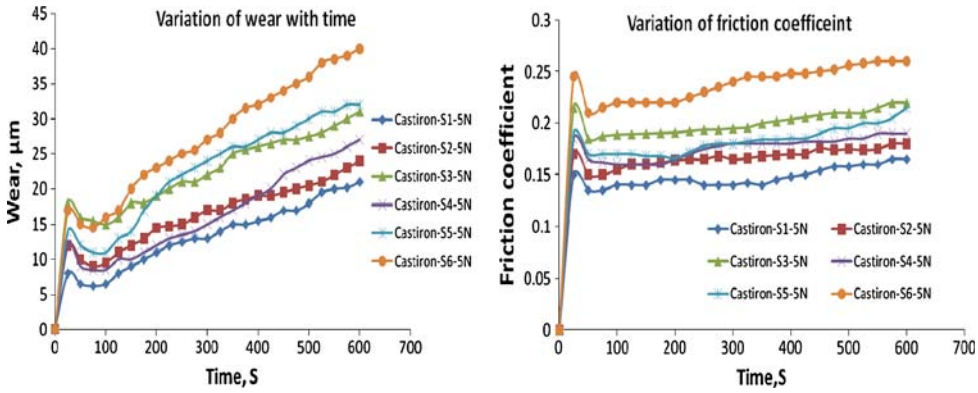

Fig. 5 Variation of wear and friction coefficient with time under 5 N load

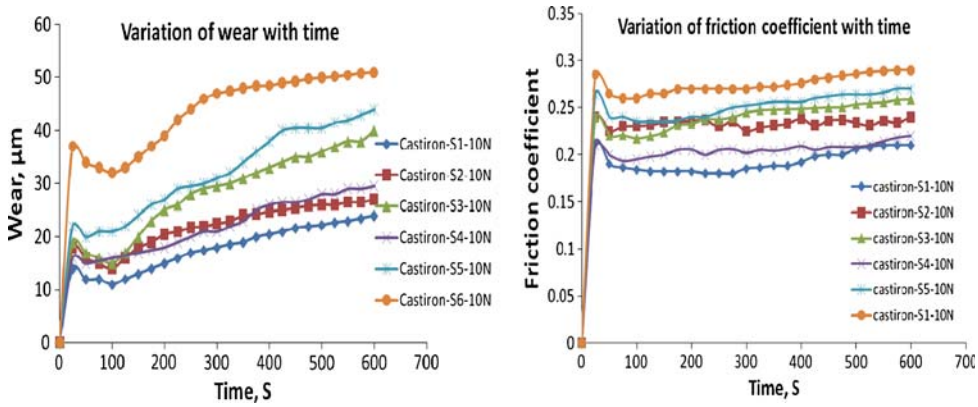

Fig. 6 Variation of wear and friction coefficient with time under 10 N load

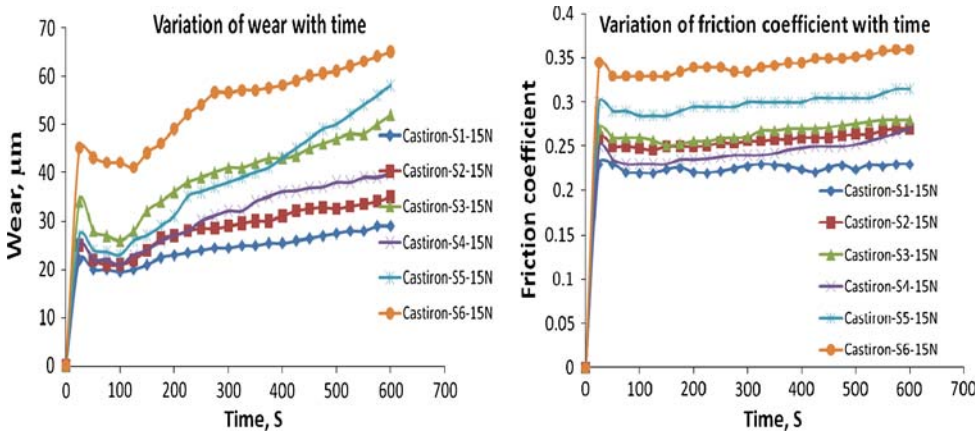

Fig. 7 Variation of wear and friction coefficient with time under 15 N load

testing, the increase in coefficient of friction is more frequent, due to the initial roughness of the two surfaces in contact. The SEM micrographs of as-sprayed coatings in Fig. 2 show that the top coat possesses semi-molten and unmolten splats. Wear debris is generated from these particles during running-in-period. Thus, the process of wear after the initial running-in-step becomes a case of three body abrasion rather than two body sliding with the release of wear debris. This is the main reason for the rise in coefficient of friction. It may be also due to the removal of hard reinforcement from the comparatively soft matrix. Such ploughing action likely causes an increase in tangential forces, in turn increasing the coefficient of friction. The decrease in coefficient of friction in the next step is due to smoothening of top coat hard particles that are not removed during first step and this produces a glazed surface. From this stage onwards the friction coefficient more or less same until the top coat is removed. Now the bond coat of the specimen comes in contact with the disk. Since the bond coat material is soft, material is removed rapidly from the specimen by increasing the coefficient of friction. The SEM micrographs of worn surfaces show that the maximum portion of top coat is removed exposing bond coat in S3 and S4 under 5 N, S1 and S2 under 10 N

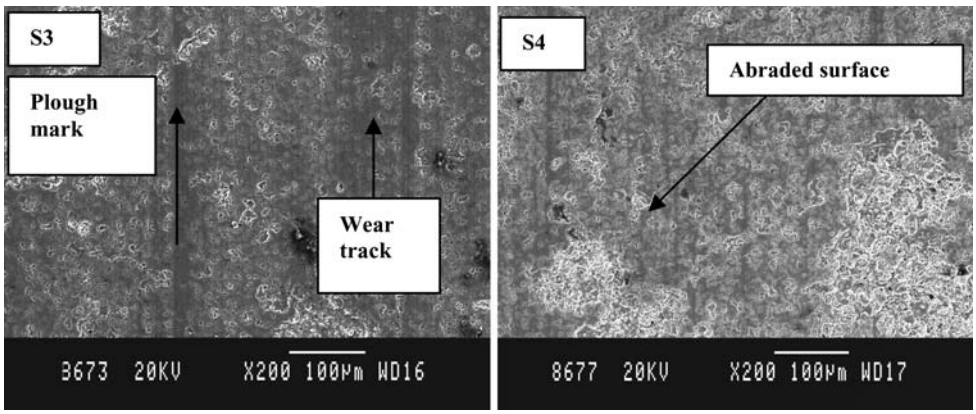

Fig. 8 SEM micrographs of worn surface for S3 and S4 under 5 N loads

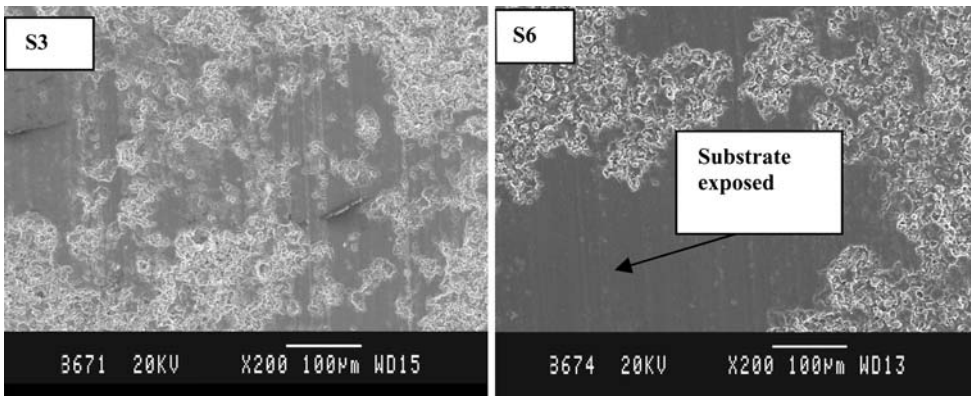

Fig. 9 SEM micrographs of worn surface for S3 and S6 under 10 N loads

load in Figs. 8 and 10, respectively. S3 and S6 in Fig. 9, S4 and S6 in Fig. 10 show the delamination of maximum portion of the bond coat from the substrate. Thus the trend of the graph in Figs. 5, 6, and 7 can be correlated with the SEM micrographs of worn surfaces of the coating in Figs. 8, 9, 10. (SEM micrographs are shown only for few samples. Similar trend is obtained for the other samples).

From Figs. 5, 6, and 7, it is observed that coefficient of friction increases with increase in the load. This is mainly due to increase in contact area with respect to load. It is also observed that in many cases friction coefficient has been increased with increase in top coat thickness. It is mainly due increase in porosity and roughness with respect to coating thickness [35]. It is also observed that the coefficient of friction is more for $ZrO_2$5CaO coatings as the roughness of these coatings is little bit high.

Figures 5, 6, 7 show the variation of wear with time. It is observed that there is a very short period of an increase in wear followed by a decrease. After this, wear gradually increases till the end of the test. The reason for sudden increase in wear during running in step is similar to that explained for coefficient of friction. The decrease in the wear after running in step is mainly due to the combined polishing and abrading of hard Al_2O_3 particles of the coating with the disk material. Further increase in the wear is due to the removal of top coat remaining which has been completely cracked during the previous stage. From the graphs, it is found that wear increases with increase in load and top coat thickness. It is also observed that the wear of $ZrO_2$5CaO coatings is more than that of Al_2O_3 coatings which is mainly due to their high porosity, dense structure of microcracks as noticed in SEM micrographs (Fig. 2). The wear rates are calculated as the volume loss per unit of applied load and unit of sliding distance. The wear rate of samples S1, S2, S3 with Al_2O_3 top coat and samples S4, S5, S6 with $ZrO_2$5CaO top coat under 15 N loads is $0.8642 \times 10\ e^{-3}$, $1.34 \times 10\ e^{-3}$, $1.267 \times 10\ e^{-3}$, $1.45 \times 10\ e^{-3}$, $1.645 \times 10\ e^{-3}$, and $1.876 \times 10\ e^{-3}$ mm^3/Nm, respectively.

Wear mechanism

The wear tracks for 5, 10, and 15 N loads are shown in Figs. 8, 9, 10. The micrographs of the worn surfaces indicated that the wear is taking place mainly by abrasion mechanism. The width of the wear track is observed to increase with the increase in load. This is clearly due to the increase in the initial contact area as the load increases. Plough marks are observed in the wear tracks. The 15 N load wear track appears to have deeper plough marks than the 10 and 5 N tracks. This is mainly due to that a particle trapped between the harder disk material and soft coating

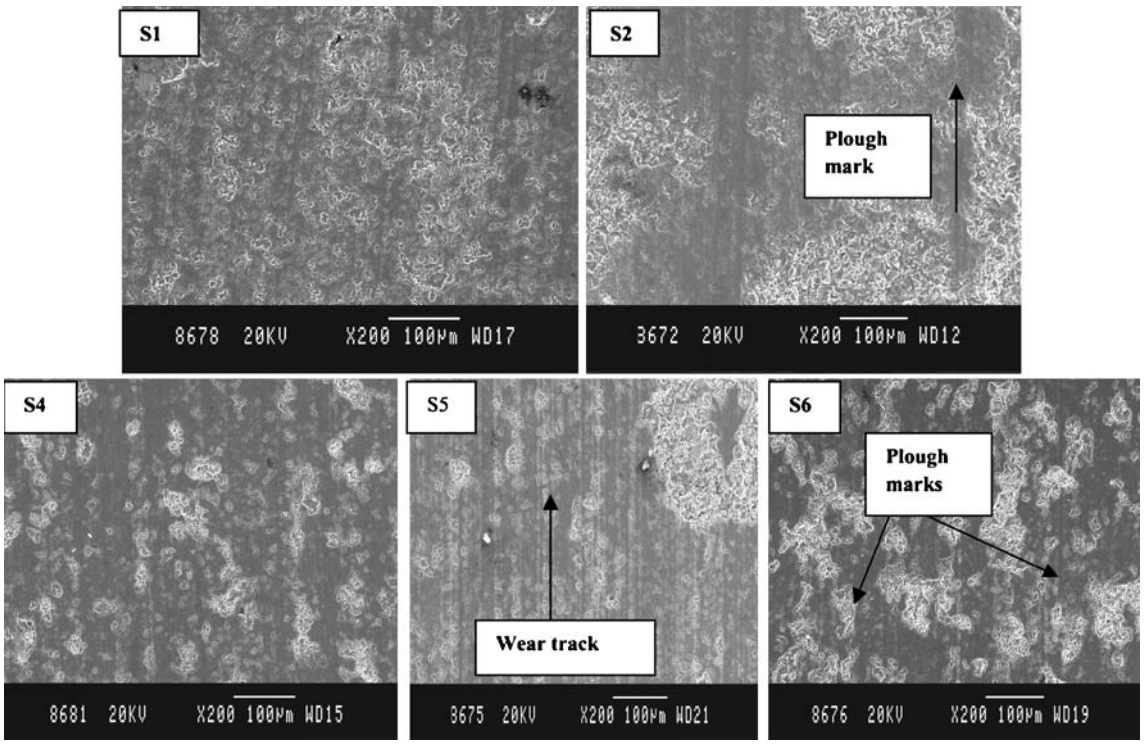

Fig. 10 SEM micrographs of worn surface for the samples S1, S2, S4, S5, and S6 under a load of 15 N

under the highest load would indent deeper into the coating and that cause deeper ploughing marks, leading greater amount of material removal. From the SEM micrographs (Figs. 8, 9, and 10) it can be seen that the dominating mechanism of material removal for the Al_2O_3 and ZrO_2 5CaO coatings is the combination of grain dislodgement due to grain boundary fracture and lateral crack chipping. It is commonly indicated that the wear resistance of material is closely related to its micro hardness, toughness, microstructure, defect coating, and the ratio of its hardness to the hardness of the abrasive [36–41]. From the literature, it is found that, high hardness is desirable for both brittle and ductile materials while a brittle material benefits further from improved toughness [36, 42], but wear is a complex process that many factors will influence it. In certain cases one or more factors will dominate wear resistance of the material. In addition to the effect of toughness and hardness, the microstructure of ceramics especially grain size has an immense influence on the wear resistance.

Conclusions

In this study, two plasma-sprayed oxide ceramic coatings, namely Al_2O_3 and $ZrO_2$5CaO have been characterized in terms of microstructure and wear properties. The experimental results lead to the following conclusions.

1. The average roughness of Al_2O_3 and $ZrO_2$5CaO coatings lies in the range of 3.5–5.5 µm and 4.5–6.8 µm, respectively.
2. The increase in top coat thickness slightly increases the roughness as well as porosity. The porosity of $ZrO_2$5CaO coatings was slightly greater than that of Al_2O_3 coatings.
3. The observed increase in coefficient of friction is mainly due to 3-body abrasion with the release of wear debris.
4. Coefficient of friction and wear mainly depends on loading conditions. Initially, mechanism of wear is mainly due to abrasion and once the bond coat is exposed to the disk, it loses material by adhesion.
5. It was found that the coefficient of friction and wear for ZrO_2CaO coatings is more than that of Al_2O_3 coatings.
6. The results obtained showed that the pin-on-disk test was able to discern the effects of the changes in the imposed test conditions.

References

1. Bhushan B, Gupta BK (1991) Handbook of tribology—materials, coatings and surface treatments. McGraw-Hill, New York, p 1168
2. Yonushonic TM (1989) Thermal spray technology, new ideas and processes. ASM International, Metals Park, OH, pp 239–243

3. Novak RC, Matarese AP, Huston RP (1989) Thermal spray technology, new ideas and processes. ASM International, Metals Park, OH, pp 273–281
4. Guillemot JM, Dehaudt P, Ducos M (1986) Proceedings of 11th international thermal spraying conference, Pergamon Press, New York, pp 513–521
5. Inwood BC, Meyer, Grunow H, Chandler PE (1989) Proceedings of 12th thermal spraying conference, paper 91, vol 1. The Welding Institute, Cambridge
6. Sheppard LM (1990) Am Ceram Soc Bull 69:1012
7. Miller RA (1991) EPRI Report, AP-5078
8. Handbook of thermal spray technology, ASM International, Materials Park, OH, USA, 2003–2004, p 171
9. Ko PL, Robertson MF (2002) Wear 252:880
10. Rastegar F, Richardson DE (1997) Surf Coat Technol 90:156
11. Tucker RC (2002) Int J Powder Metall 38:45
12. Westergard R, Erickson LC, Axen N, Hawthrone HM, Hogmark S (1998) Tribol Int 31:271
13. Yoma D, Brandl W, Marginean G (2001) Surf Coat Technol 138:149
14. Fu YQ, Batchelor AW, Wang Y, Khor KA (1998) Wear 217:132
15. Liao H, Normand B, Coddet C (2000) Surf Coat Technol 124:235
16. Heimann RB (1996) Key Eng Mater 122–124:399
17. Herman H, Sampath S, Stern KH (1996) Metallurgical and ceramic protective coatings. Chapman and Hall, London, p 263
18. Barbezat G, Nicoll AR, Sickinger A (1993) Wear 162–164:529
19. Ramnath V, Jayaraman N (1989) Mater Sci Technol 5:382
20. Fernandez JE, Rodriguez R, Wang Y, Vijande R, Rincon A (1995) Wear 181–183:417
21. Kamo R, Assanis DN, Bryzik W (1989) Thin thermal barrier coatings for engines. Trans SAE, Paper No. 890143, pp 131–139
22. Miyains V, Matsuhisa T, Ozawa T (1989) Selective heat insulation of combustion chamber walls for a DI diesel engine with monolithic ceramics. Trans SAE, Paper No. 890141, pp 117–129
23. Kamo R (1997) Coatings for improving engine performance. Trans SAE, section-3, Paper No. 970204, pp 354–363
24. Vittal M, Borek JA (1999) Trans ASME 121:218
25. Hejwowski T, Weronski A (2002) Vacuum 65:427
26. Prasad R, Samria NK (1989) Int J Mech Sci 31:10
27. Xie Y, Hawthrone HM (1999) Wear 233–235:293
28. Xie Y, Hawthrone HM (1999) Wear 225–235:90
29. Erickson LC, Hawthrone HM, Troczynski T (2001) Wear 250:569
30. Budinsky KG (1995) Wear 181–183:938
31. Bolelli G, Cannilio V, Lusvarghi L, Ricco S (2006) Surf Coat Technol 200:2995
32. Niemi K, Sorsa P, Vouristo PP, Mantyla T (1994) Proceedings of 7th international thermal spraying conference, Massachusetts, p 533
33. Abdel-Samad AA, El-Bahloul AMM, Lugscheider E, Rassoul SA (2000) J Mater Sci 35:3127. doi:10.1023/A:1004824104162
34. Knuutila J, Ahmaniemi S, Leivo E, Sorsa P, Vuoristo PP, Mantyla T (1998) Proceedings of 15th international thermal spraying conference, France, p 145
35. Sarikaya O (2005) Surf Coat Technol 190:388
36. Wang Y, Jiang S, Wang S, Xiao TD, Strutt PR (2000) Wear 237:176
37. Tabor D (1997) Wear-A critical synoptic view. In: Glaeser WA et al (eds) Wear of materials. ASME, New York, p 1
38. Chu SJ, Moon H, Hockey BJ, Hsu SM (1992) Acta Metall Mater 40:185
39. Ramalingam S, Wright PK (1981) J Eng Mater Technol 103:151
40. Boas M, Bamberger M (1988) Wear 126:197
41. Khruschov MM (1974) Wear 28:49
42. Chu SJ, Hockey BJ, Lawn BR, Bennison SJ (1989) J Am Ceram Soc 72:1249